PLOS ONE

RESEARCH ARTICLE

Separating the effects of temperature and carbon allocation on the diel pattern of soil respiration in the different phenological stages in dry grasslands

János Balogh[1]*, Szilvia Fóti[1,2], Marianna Papp[1,2], Krisztina Pintér[1,2], Zoltán Nagy[1,2]

1 Institute of Botany and Ecophysiology, Szent István University, Gödöllő, Hungary, **2** MTA-SZIE Agroecology Research Group, Szent István University, Gödöllő, Hungary

* balogh.janos@mkk.szie.hu

Citation: Balogh J, Fóti S, Papp M, Pintér K, Nagy Z (2019) Separating the effects of temperature and carbon allocation on the diel pattern of soil respiration in the different phenological stages in dry grasslands. PLoS ONE 14(10): e0223247. https://doi.org/10.1371/journal.pone.0223247

Editor: Débora Regina Roberti, Universidade Federal de Santa Maria, BRAZIL

Received: January 30, 2019

Accepted: September 17, 2019

Published: October 17, 2019

Data Availability Statement: All supporting files are available from the Figshare repository (https://figshare.com/s/12744b8f0d1b1fc56bab, https://figshare.com/s/0f1ac5e2889f59d82775, https://figshare.com/s/16c0eebe1fe81234e7db).

Funding: This research was supported by the Higher Education Institutional Excellence Program (TUDFO/47138/2019-ITM) awarded by the Ministry of Innovation and Technology of Hungary within the framework of water related researches of Szent István University. Soil respiration measurements

Abstract

Diel variability of soil respiration is influenced by several factors including temperature and carbon allocation as the most significant ones, co-varying on multiple time scales. In an attempt to disentangle their effects we analyzed the dynamics of soil respiration components using data from a three-year soil respiration study. We measured CO_2 efflux in intact, root-excluded and root- and mycorrhizal fungi excluded plots and analyzed the diel variability in different phenological stages. We used sine wave models to describe the diel pattern of soil respiration and to disentangle the effects of temperature from belowground carbon allocation based on the differences between component dynamics inferred from the fitted models. Rhizospheric respiration peaked 8–12 hours after GPP peak, while mycorrhizal fungi respiration had a longer time lag of 13–20 hours. Results of $\delta^{13}CO_2$ isotopic signals from the respiration components showed similar patterns. It was found that drought affected the component respiration rates differently. Also, the speed and the amount of carbon allocation to the roots as well as to the mycorrhizal fungi was reduced under drought. We conclude that the diel variability of soil respiration is the result of the integrated patterns of temperature- and carbon allocation-driven components in dry grasslands and their share depends on their phenological stages and stress state.

Introduction

The carbon balance of ecosystems is the sum of sink and source activities and exhibit large seasonal and interannual variability [1]. Since the major part of the source activity is the result of soil respiration (R_s), the variability of this CO_2 flux has a significant relevance in the carbon balance [2]. Soil respiration is a highly complex process including a wide range of soil biota (autotrophic and heterotrophic functioning) and different pathways of carbon cycling (decomposition, carbon allocation), all being under the control of environmental and biotic drivers [3–5]. Improving our understanding of the links between these processes and their drivers on

were also supported by OTKA-PD 100575 project. Szilvia Fóti and Krisztina Pintér acknowledge the support of GINOP-2.2.1-15-2017-00061 project. János Balogh acknowledges the support of 2017-1.3.1-VKE-2017-00030 project. The funders had no role in study design, data collection and analysis, decision to publish, or preparation of the manuscript.

Competing interests: The authors have declared that no competing interests exist.

multiple time scales has a major importance in decreasing uncertainties concerning the carbon cycle models of ecosystems [6] as well as in decreasing uncertainties related to ecosystem respiration estimations [7].

Drought-prone ecosystems are key members of the global carbon cycling contributing significantly to the interannual variability of the global CO_2 sink [8]. Their carbon balance is strongly associated with the variations in precipitation and temperature and can turn from carbon sink to carbon source due to drought [9,10]. Dry grasslands, often subjected to drought, experience strong seasonality and their functioning depends upon the presence and activity of the canopy [11,12]. Therefore, the coupling between aboveground gross primary productivity (GPP) and carbon allocation to roots and root-associated organisms varies depending on the season [13]. The vegetation type defines the phenological stage and the range of productivity on a seasonal scale, as well as the coupling of photosynthesis and belowground respiration on the diel scale [3,14]. Seasonality induces changes in belowground carbon allocation patterns with the amounts of carbon allocated to the roots and to the mycorrhizal fungi partners being highly variable in the different seasons [15,16] and the use of fresh assimilates for respiration or storage also depending on the phenological stage [17].

The major factor hampering the quantification of the carbon allocation driven part of soil respiration is the temperature co-varying with GPP on seasonal and diel time scales [13,18,19]. The sole effect of temperature on R_s was extensively studied [20,21] and the correlation was used as a basis for soil respiration models but potential artefacts were already highlighted as well [7,22]. The observed time lag between soil temperature and R_s and the diel variation of R_s was often attributed to the depth at which temperature was measured [23,24] or to the gas transport properties of the soil [25] combined with other factors [3,26]. Furthermore, attempts were also made to explain the time lags in the different responses of soil respiration components. However, changes in R_s can even precede those occurring in soil temperature especially in dry ecosystems [27,28].

Generally, the autotrophic component of R_s is determined by the amount of CO_2 produced by plant roots and associated microorganisms (rhizospheric microbes, mycorrhizal fungi), while heterotrophic respiration is represented by the amount of CO_2 produced by microbial decomposition of SOM [29]. R_s partitioning could be useful for estimating the contribution of the different components and for revealing the potential effects of the drivers on the autotrophic and heterotrophic components of the soil. Heterotrophic activities were found to be more sensitive to temperature than the autotrophic ones [19,30], while less sensitive to drought conditions [31], although the responses can vary with the type of vegetation [32]. However, both autotrophic and heterotrophic components receive assimilates from the shoots [33,34], therefore the dynamics of belowground carbon allocation should also be included in the analysis of component responses.

Our objective was to characterize the diel patterns of the temperature and carbon allocation driven parts of soil respiration and their changes in the different phenological stages. In our attempt to do so, we analyzed the diel variability of soil respiration as well as the CO_2 efflux of root-excluded and root- and mycorrhizal fungi-excluded plots in three consecutive years. Measurements of $\delta^{13}C$ were also conducted together with the CO_2 efflux measurements in the growing season in one of the study years. Significant drought periods intervened in the growing seasons in two of the studied years allowing us to analyze the effect of drought on the diel pattern of soil CO_2 efflux.

Our analysis focused on the (1) differences in time lags between GPP and the respiration components; and the (2) share of the carbon allocation driven part in soil respiration in the different phenological stages. We hypothesize that it is the diel dynamics of carbon allocation that drive a significant part of soil respiration in the growing season and it is influenced by the

drought periods resulting in seasonally different diel patterns. We also hypothesize that the time lag between GPP and respiration is longer in mycorrhizal fungi than in roots and rhizosphere due to the allocation patterns within the soil.

Methods

Site description

The vegetation at the Bugac site (46.69˚ N, 19.6˚ E, 114 m above sea level) is a dry sandy grassland dominated by *Festuca pseudovina*, *Carex stenophylla* and *Cynodon dactylon* and it has been under extensive management (grazing) for the last 20 years [35]. The ten-year mean annual precipitation (2004–2013) was 575 mm and the mean annual temperature reached 10.4 ˚C. According to the FAO classification [36] the soil type is Chernozem with a relatively high organic carbon content, the soil texture is a sandy loam with a sand:silt:clay ratio of 81:11:8% in the topsoil layer [37].

Measured and calculated CO_2 efflux components

In September 2010 ten soil cores (160 mm in diameter and 800 mm in depth, except No. 9, which had 500 mm diameter) were drilled and the roots have been removed by sieving. During the drilling 4 soil layers were separated: 0–10 cm, 10–30 cm, 30–50 cm and 50–80 cm The root-free soil was packed layer by layer into PVC tubes. Five tubes were used to exclude both roots and mycorrhiza. Walls of another 5 tubes were partially removed and replaced by inox meshes (40 μm pore size) to exclude roots, while ensuring that the mycorrhiza filaments can grow into the tubes [38]. These root- and mycorrhiza free and only root-free soil cores were placed at a distance of 6 m from the eddy covariance tower to South (S1 Fig). The distance between the soil cores/tubes was 50 cm.

Soil CO_2 efflux and its isotopic signal were measured in plots of:

- undisturbed soil: soil respiration, R_s,
- root-excluded soil = without roots but with arbuscular mycorrhizal fungi, $R_{basal+myc}$.
- soil without roots and arbuscular mycorrhizal fungi = basal respiration, R_{basal},

The presence of mycorrhizal fungi filaments in $R_{basal+myc}$ and R_s plots was confirmed by microbiological investigations as well as overall soil enzymatic activity measured in all plots [39].

Although it was not possible to calculate the respiration rates of the autotrophic and heterotrophic components directly, we used the differences between the average respiration rates of specific plots for describing the diel pattern of the components of soil respiration. According to our approach we calculated the respiration components as follows:

- mycorrhizospheric component [29]:

$$R_{myc+rhizo} = R_s - R_{basal} \quad (1)$$

- mycorrhizal fungi component:

$$R_{myc} = R_{basal+myc} - R_{basal} \quad (2)$$

- rhizospheric component:

$$R_{rhizo} = R_s - R_{basal+myc} \quad (3)$$

Table 1. Measured and calculated components of soil respiration used in this study.

	Abbreviation	Description	Priming included
Measured	R_s	soil respiration, containing all of the components, measured in undisturbed soil	yes
	$R_{basal+myc}$	basal and mycorrhizal fungi respiration, measured in root-excluded soil	partly
	R_{basal}	basal respiration, respiration of SOM decomposition without the priming effect	no
Calculated	$R_{myc+rhizo}$	respiration of roots, rhizosphere microorganisms and mycorrhizal fungi	yes
	R_{rhizo}	respiration of roots and rhizosphere microorganisms	partly
	R_{myc}	respiration of mycorrhizal fungi filaments	partly

https://doi.org/10.1371/journal.pone.0223247.t001

Table 1 contains the description of measured and calculated soil respiration components and abbreviations used in the study following the terminology of Moyano et al. [29]. Priming effect was not partitioned, therefore it was included in the respective $R_{myc+rhizo}$, R_{myc} and R_{rhizo} components.

Gas exchange measuring systems

Different gas exchange systems were used in the present study: eddy-covariance system (EC), automated soil respiration measuring system (SRS) and an isotopic CO_2 analyzer (cavity ring-down spectroscopy, CRDS-technique) was connected to the SRS in 2013 (see Isotopic measurements). The size of the EC flux footprint area was larger by several orders of magnitude than the area covered by the SRS. Care was taken during the establishment of the experiment to install the partitioning set-up with the same average soil characteristics and vegetation composition and cover as found in the EC footprint area [35]. Hence, the NEE and GPP estimates obtained in this way can be considered to be representative also of the small-scale SRS and isotope measurements.

Data from 6th July 2011 to 12th May 2014 were analyzed in this study.

Eddy-covariance setup

The EC system at the Bugac site has been measuring the CO_2 and sensible and latent heat fluxes continuously since 2002. In dry years the grassland can turn into a net carbon source [9], but the longer-term annual sums of net ecosystem exchange (NEE) show it to be a net sink, ranging from –171 to +106 g C m^{-2} yr^{-1} [40,41] with a -100 g C m^{-2} yr^{-1} average.

The EC system consists of a CSAT3 sonic anemometer (Campbell Scientific, USA) and a Li-7500 (Licor Inc, USA) open-path infra-red gas analyzer (at the height of 4 m, anemometer direction: north), both connected to a CR5000 data logger (Campbell Scientific, USA) via an SDM (synchronous device for measurement) interface. Additional measurements used in the present study included air temperature and relative humidity (HMP35AC, Vaisala, Finland), precipitation (ARG 100 rain gauge, Campbell, UK), global radiation (dual pyranometer, Schenk, Austria from 2002 and CMP3, Kipp&Zonen, The Netherlands from 2013) incoming and reflected photosynthetically active radiation (SKP215, Campbell, UK), volumetric soil moisture content (CS616, Campbell, UK) and soil temperature (105T, Campbell, UK). Surface temperature (T_{surf}) was measured by 3 cm above the ground under the leaves. These measurements were performed as described by Nagy et al. and Pintér et al. [9,40]. Fluxes of sensible and latent heat and CO_2 were processed by EddyPro® [42] using double rotation, linear detrending and WPL correction [43]. Gap-filling and flux partitioning was performed by the REddyProc online data processing tool [44].

Soil respiration system

Automated soil respiration system consisting of ten chambers was set up in July 2011. The system is an open dynamic one, consisting of an SBA-4 infrared gas analyzer (PPSystems, UK), pumps, flow meters (D6F-01A1-110, Omron Co., Japan), electro-magnetic valves, and PVC/metal soil chambers. The chambers were 10.4 cm high with a diameter of 5 cm, covering a soil surface area of 19.6 cm^2. The flow rate through the chambers was 300 ml min^{-1}, exchanging the air in the chamber in 40 seconds. The PVC chambers were enclosed in a white metal cylinder with 2 mm airspace in between to stabilize the chamber and to prevent warming by direct radiation. Four vent holes with a total area of 0.95 cm^2 were drilled in the top of the chambers. Vent holes also served to allow precipitation to drip into the chambers. The system causes minor disturbances in the soil structure and the spatial structure of the vegetation. It can be applied without cutting the leaves/shoots of the plants, so it does not disturb the transport processes taking place within the plant stems and roots. It is suitable for continuous and long-term unattended measurements of soil CO_2 efflux and was used in previous experiments [45]. The soil respiration chambers contained no standing aboveground plant material.

Measurements with the SRS chambers were carried out as follows: R_s was measured by 6 SRS chambers within the area in random positions (cf. S1 Fig), $R_{basal+myc}$ was measured by 2 SRS chambers in plots of PVC tubes with inox mesh and R_{basal} was measured by 2 SRS chambers in intact PVC tubes. Positions of the chambers were changed every 2 weeks within the corresponding treatments during the study period that is among the 10 tubes ($R_{basal+myc}$, R_{basal}) or among randomly selected locations within the undisturbed area (R_s) to obtain sequential spatial replications for each treatment type. The system operated in sequential mode during the whole study period: it was idle after one hour of operation, during which the chambers were measured twice (two cycles of measurements). Despite the vent holes in the chambers there was a build-up of CO_2 concentration within the chambers before the system was idle, therefore the data recorded in the first 30 minutes (first cycle) was excluded from the analysis. One measurement of each chamber lasted 3 minutes with the reference/analysis air being switched in every 7 seconds. This procedure resulted in 12 measurements (36 min)/day for each chamber.

Two soil moisture and soil temperature sensors (5TM, Decagon Devices, USA) were also attached to the system measuring soil temperature and moisture of an R_s plot (T_{Rs}) and an R_{basal} plot (T_{Rbasal}) at a depth of 5–9 cm.

Isotopic ($^{13}CO_2$) measurements

A Picarro G1101-i gas analyzer (Picarro Inc., CA, USA) was attached to the soil respiration system from 15th May to 12th November in 2013. Since the CRDS had much slower response than the SRS, every second chamber of the SRS was measured by the CRDS. Out of these five chambers, 3 chambers measured R_s, one of them measured $R_{het+myc}$ and one of them measured R_{het}. Regularly changing the position of the chambers ensured the spatial replications of the measurements [31].

The CRDS system measured the isotopic composition of the reference air (in the grass canopy 10 cm above the surface) when the soil respiration system was idle and between two chamber measurements. Similarly to the SRS, one chamber was measured for 3 minutes. After each chamber the isotopic signal of the reference air was measured for 3 minutes. The procedure gave a sequence of reference and analysis (soil CO_2 efflux as sampled from the chamber) air for 3–3 minutes in one hour of operation.

Data processing and modelling

Data processing and statistical analysis were done in R [46]. Gaussian error propagation was used to calculate propagated uncertainties for the averages and model parameters.

Diel patterns of respiration for R_s, $R_{basal+myc}$, R_{basal}, $R_{myc+rhizo}$, R_{myc} and R_{rhizo} were modeled using a sine wave function [13]:

$$R = y0 + a \times sine\left[\left(\frac{2 \times \pi \times TOD}{2400}\right) + c\right] \quad (4)$$

where *y0* represents the mean respiration rate over the time period modeled (μmol CO_2 m^{-2} s^{-1}), *a* is diel amplitude (μmol CO_2 m^{-2} s^{-1}), *c* corresponds to the shift of minimum and maximum diel peaks (radians), and *TOD* is time of day in hundreds. Using parameter *c* we calculated the peak timing of respiration (PTR).

The goodness of model fit was quantified by the Nash–Sutcliffe model efficiency (NSE) coefficient, which is calculated similarly to the coefficient of determination, but ranges from -∞, indicating a better prediction of the observed values by the mean than by the model to 1, which points to a perfect match of the observed and modelled data.

We assumed that diel changes of R_{basal} were mainly driven by the temperature, since this plot had no connection with living plants. We also assumed that the diel pattern of $R_{myc+rhizo}$, R_{myc} and R_{rhizo} was governed by the carbon allocation, because the temperature response was removed by the subtraction of R_{basal}. Therefore, we used some parameters obtained from fitting Eq 4 on the component's respiration pattern in order to estimate the temperature and carbon allocation driven part of soil respiration.

The following additive model (Eq 5) was a conceptual framework for the estimation of the actual share of the temperature driven response and of the potential diel course of the carbon allocation driven part of soil respiration.

Sine wave models were combined into an additive model in order to estimate the effects of temperature and carbon allocation on the respiration, as follows:

$$R_s = \left\{y1 + a_{Rbasal} \times sine\left[\left(\frac{2 \times \pi \times TOD}{2400}\right) + c_{Rbasal}\right]\right\} + \left\{(1 - y1) + a1 \times sine\left[\left(\frac{2 \times \pi \times TOD}{2400}\right) + c_{Rmyc+rhizo}\right\}\right] \quad (5)$$

where a_{Rbasal} is the amplitude (a, μmol CO_2 m^{-2} s^{-1}) and c_{Rbasal} is the diel peak (c, radians) from the fitted Eq 4 on R_{basal} dataset, *y1* is the mean temperature driven part of soil respiration (μmol CO_2 m^{-2} s^{-1}), $c_{Rmyc+rhizo}$ is the diel peak (radians) from the fitted Eq 4 on $R_{myc+rhizo}$ dataset and *a1* is the amplitude of the carbon allocation driven part of R_s (μmol CO_2 m^{-2} s^{-1}) in the corresponding phenological period. In the first term of Eq 5 we used two model parameters of Eq 4 fitted on R_{basal} (*a* and *c*) for estimating the temperature response within soil respiration, while parameter *y1* was allowed to vary. In the second term of Eq 5 we estimated the carbon allocation driven part of soil respiration, only the diel peak of $R_{myc+rhizo}$ ($c_{Rmyc+rhizo}$) was kept constant with *a1* being allowed to vary.

We also used GPP data and the calculated components of soil respiration to calculate Pearson correlation coefficients at different time lags using ccf function (cross-correlation) of R.

During the isotopic measurements the reference and chamber air were measured sequentially, therefore reference values during chamber measurements were estimated by linear interpolation between the neighboring reference sequences.

$\delta^{13}C$ values of the soil CO_2 efflux were calculated using the isotopic mass balance approach in each plot:

$$\delta^{13}C_R = \frac{\delta^{13}C_{out} \times c_{out} - \delta^{13}C_{in} \times c_{in}}{c_{out} - c_{in}} \quad (6)$$

where $\delta^{13}C_{out}$ and $\delta^{13}C_{in}$ are the isotopic signature of the outgoing and incoming air of the chamber and c_{out} and c_{in} are the CO_2 concentration of the of the outgoing and incoming air of the chamber, respectively.

$$\delta^{13}C = \frac{R_{sample}}{R_{standard}} - 1 \quad (7)$$

and *R* stands for the ^{13}C:^{12}C isotope ratio of the sample and the international VPDB standard (0.011182), respectively.

For the details of data processing of isotopic measurements see Balogh et al. [31].

Results

Meteorological conditions, CO_2 uptake and respiration rates among years and phenological periods

The annual sums of precipitation in 2011 and 2012 were lower (436 and 431 mm $year^{-1}$, respectively) than the ten–year average (575 mm), while it was close to that in 2013 (590 mm) and higher in 2014 (806 mm). Despite the low sum of precipitation in 2011 the grassland acted as a sink of carbon and no drought period could be distinguished within this year (Fig 1). The good water availability during the summer period in 2011 was due to the large amount of precipitation in 2010 (annual sum: 961 mm) and to the fact that 70%of the precipitation fell from March to September. This variability in water availability resulted in an overall sink activity in 2011 (-135 g C m^{-2} $year^{-1}$), source activity in 2012 (38 g C m^{-2} $year^{-1}$) and weak sink activity in 2013 and 2014 (-64 and -35 g C m^{-2} $year^{-1}$, respectively).

We distinguished 4 phenological stages (active, drought, fall and dormant) within each year of the study period according to the net ecosystem exchange (NEE), air temperature (T), soil water content (SWC) and normalized difference vegetation index (NDVI) variations (Fig 1). The active periods were characterized by strong sink activity, while the drought periods showed strong source activity together with decreasing NDVI, high T and low SWC. The ecosystem showed a second or fall active period after the summer but this period was marked by weak source activity according to the cumulative NEE due to the decreasing temperature and NDVI. The dormant period was characterized by low temperatures, low NDVI and weak source activity (Fig 1, Table 2).

Both R_s and $R_{basal+myc}$ decreased by 36% on average in response to drought, while R_{basal} was less responsive and decreased by 26%. Average R_s and $R_{basal+myc}$ were higher by 65% and 33% than R_{basal} in the active period and by 43% and 14% in the drought period, respectively. Average R_s and $R_{basal+myc}$ were also higher than R_{basal} in the fall and dormant periods by 49%, 15% and by 31%, 23%, respectively (Table 2).

Diel patterns of soil CO_2 effluxes among the phenological stages

Since the SRS measured soil CO_2 effluxes twelve times a day, we evaluated the diel changes in soil CO_2 effluxes by binning the data by time of day (12 bins) for each phenological period and fitted Eq 4 on the datasets. Binned averages and fitted models are shown in Fig 2. The parameters of the sine wave function differed for R_s, $R_{basal+myc}$ and R_{basal} (Fig 2, middle panel). Peak

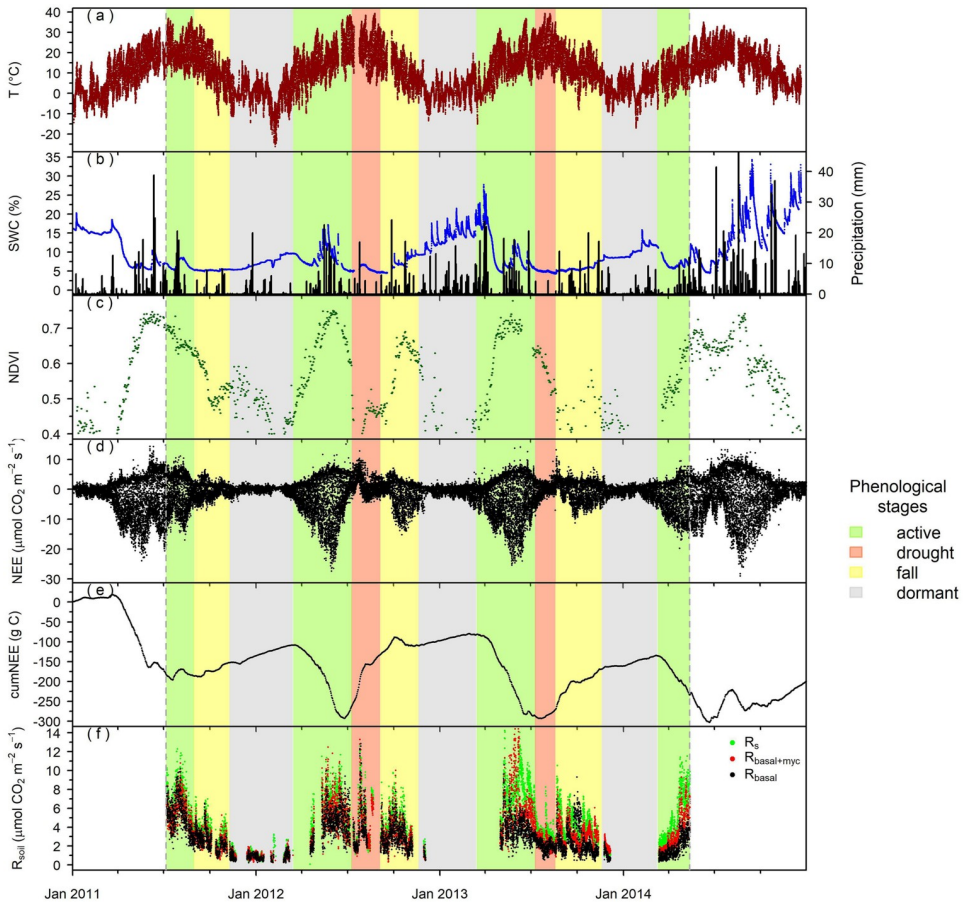

Fig 1. (a) Half-hourly average of air temperature (T, dark red dots), (b) soil water content (SWC, blue dots) at a depth of 5 cm and sum of precipitation (black bars), (c) normalized differential vegetation index (NDVI, green dots), (d) half-hourly net ecosystem exchange (NEE, black dots), (e) cumulative NEE (cumNEE, black line), and (f) hourly averages of R_s, $R_{basal+myc}$ and R_{basal} (green, red and black dots, respectively) during the study period in 2011–2014, at Bugac site. Phenological stages are shown by background colors (pale green as active, pale red as drought, yellow as fall and grey as dormant period).

https://doi.org/10.1371/journal.pone.0223247.g001

R_{basal} occurred at about 12:00–14:00 hours (local time) at all phenological stages, while peak $R_{basal+myc}$ occurred earlier in the active, drought and dormant periods (11:00–11.30). Peak R_s was observed much later than peak R_{basal} in the active period (15:30). During drought R_s peaked 4 hours earlier than in the active period and both peak R_s and $R_{basal+myc}$ (both at 11:30) preceded peak R_{basal}. Contrary to expectations, the largest amplitude (*a*) of R_s was found in the

Table 2. Average soil CO_2 effluxes (R_s, $R_{basal+myc}$ and R_{basal}), air temperature (T), soil moisture (SWC) and net ecosystem exchange (NEE) for the phenological stages of the whole study period. Standard deviations of CO_2 effluxes are shown (±SD).

Phenological stage	*R_s ($\mu mol\ CO_2\ m^{-2}\ s^{-1}$)*	*$R_{basal+myc}$ ($\mu mol\ CO_2\ m^{-2}\ s^{-1}$)*	*R_{basal} ($\mu mol\ CO_2\ m^{-2}\ s^{-1}$)*	*T (°C)*	*SWC (%)*	*NEE ($\mu mol\ CO_2\ m^{-2}\ s^{-1}$)*
active	6.25 (±1.65)	5.01 (±1.8)	3.78 (±0.98)	15.14	8.7	-1.27
drought	4.00 (±0.99)	3.19 (±0.85)	2.81 (±0.72)	22.39	5.1	1.44
fall	3.93 (±1.04)	3.03 (±0.87)	2.63 (±1.17)	12.23	7.8	0.64
dormant	1.19 (±0.38)	1.11 (±0.25)	0.90 (±0.18)	1.30	12.1	0.29

https://doi.org/10.1371/journal.pone.0223247.t002

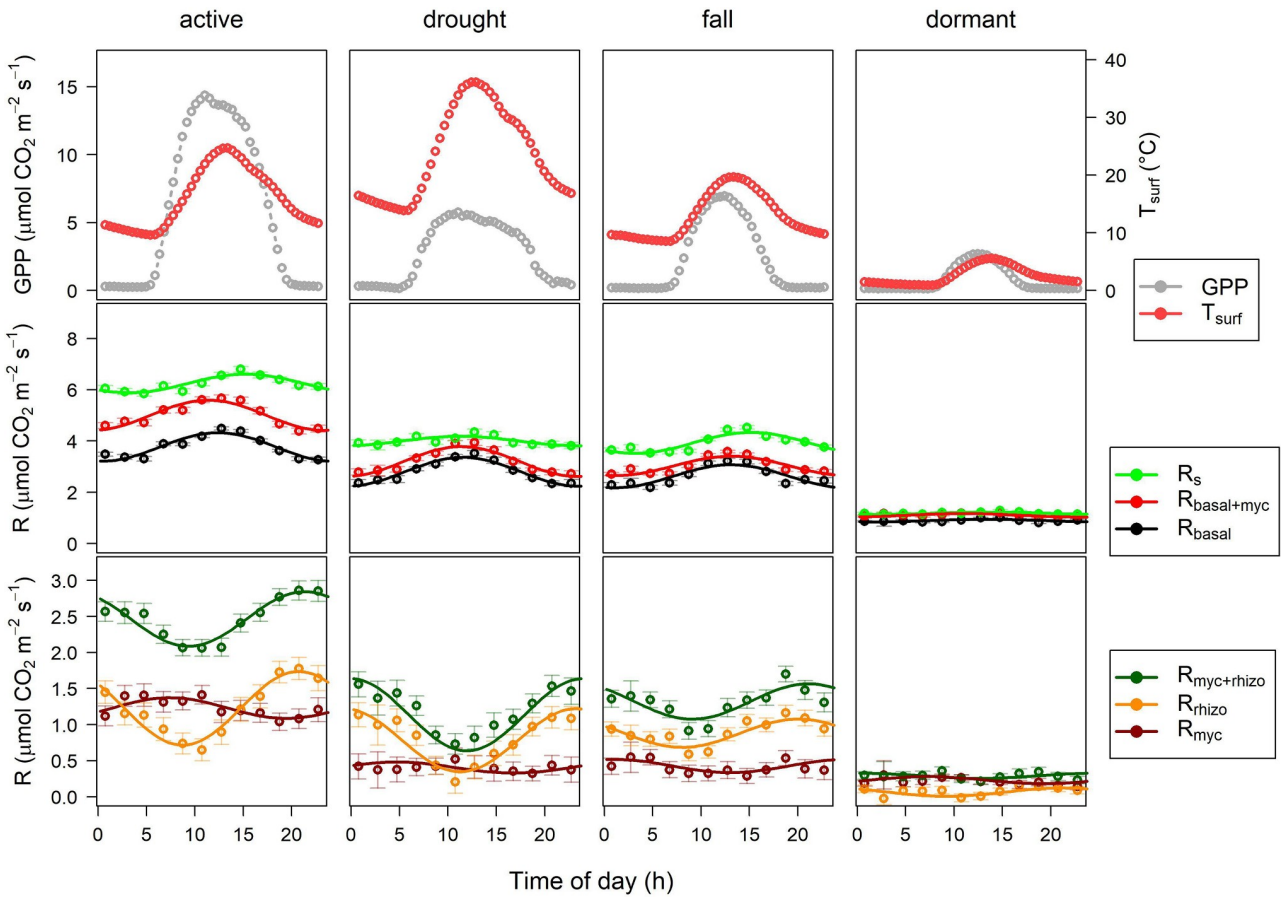

Fig 2. Diel patterns of GPP and T_{surf}, (grey and red dots, respectively, upper panel), R_s, $R_{basal+myc}$ and R_{basal} (green, red and black dots with error bars, respectively, middle panel) and R_{myc}, $R_{myc+rhizo}$ and R_{rhizo} (dark red, dark green and orange dots with error bars, y = 0 represents R_{basal}, lower panel) for the phenological stages during the whole study period at Bugac site. Lines represent fitted sine wave models (Eq 4) in middle and lower panels.

https://doi.org/10.1371/journal.pone.0223247.g002

fall period rather than in the active period. The amplitude of $R_{basal+myc}$ and R_{basal} were greater than the amplitude of R_s in the active and drought periods.

GPP was the highest at 11:15 in the active and drought periods but this peak shifted to 12:45 in the fall and dormant periods (Fig 2, upper panel). Peak R_{basal} was roughly coincident with the surface temperature (T_{surf}) peaking within the same hour (Fig 2. middle panel), except in the active period when peak R_{basal} preceded the highest temperatures by more than 1 hour.

$R_{myc+rhizo}$, R_{myc}, and R_{rhizo} showed much longer time lags with GPP (Fig 3). Peak $R_{myc+rhizo}$ occurred in the evening and at night at 21:30–1:00 by 9–12 hours after GPP peak (11:30–12:45), while R_{myc} peaked at 1:30–7.30 by 13–20 hours after GPP. R_{rhizo} peaked earlier than $R_{myc+rhizo}$ by about 0.5–1 hour (Fig 3, Table 3).

Cross-correlation results showed similar time lags with GPP. The time lag at the maximum correlation between $R_{myc+rhizo}$ and GPP was 5.5–11 hours, while a longer time lag (15–22 hours) was found between R_{myc} and GPP. The highest correlation coefficients were found in the active period at the time lags of 7.5 hours ($r = 0.27$, $P<0.001$) and 21.5 hours ($r = 0.13$, $P<0.001$) for $R_{myc+rhizo}$ and for R_{myc}, respectively.

The average diel range of respiration ($2\times a$) compared to the average respiration rate ($y0$) was the highest in R_{basal} plot (40% in drought period), while it varied between 8% (dormant) and 21% (fall) in R_s plot (Table 3, S1 Table).

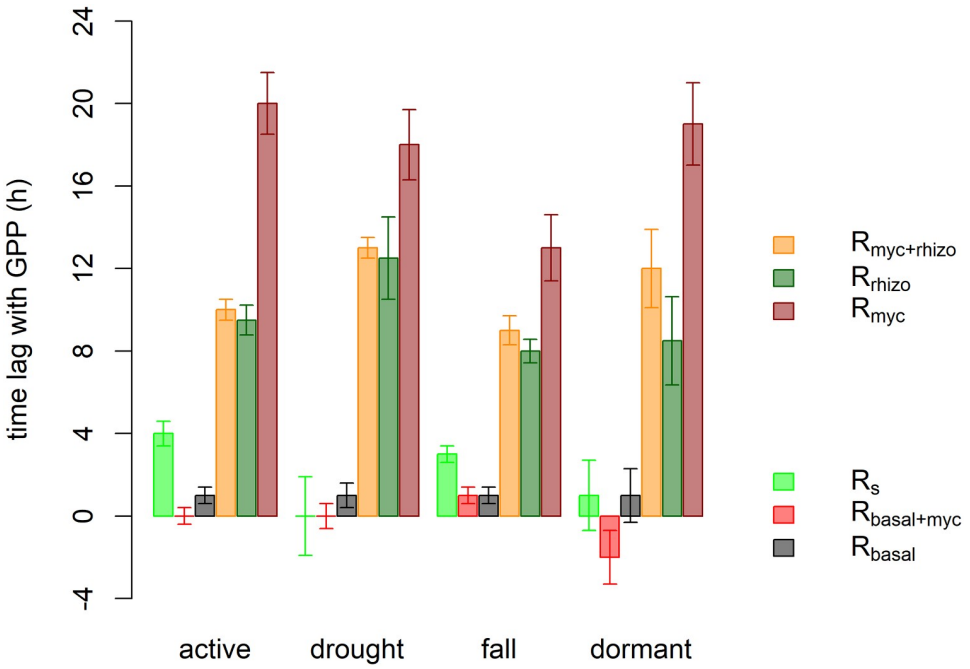

Fig 3. Average time lag between GPP peak and respiration peaks (Eq 4) in the different phenological stages. y = 0 line represents GPP peak, negative values mean that respiration preceded GPP.

https://doi.org/10.1371/journal.pone.0223247.g003

Fitting procedures of Eq 5 were successful for the active and fall periods only since *y1* parameter was not significant for the drought and dormant periods. We present here the results as a conceptual framework. The ratio of temperature and carbon allocation driven part of respiration was 0.55:0.45 in the active period, while 0.71:0.29 in fall (for the fitting results see supporting information S2–S5 Figs).

Table 3. Number of plot average values included in modelling (N), diel sine wave model parameters with propagated uncertainties (*y0*, *a*, *c* from Eq 4 (±SE)), peak timing of respiration (PTR) and Nash–Sutcliffe coefficient (NSE) for basal soil respiration component (R_{basal}), mycorrhizal fungi and rhizospheric component ($R_{myc+rhizo}$), mycorrhizal fungi component (R_{myc}) and rhizospheric component (R_{rhizo}) at phenological periods. Significance level of the parameters were P<0.001 or P<0.05 (*).

Phenol. stage	*plot*	*N*	*y0* (*μmol CO_2 m^{-2} s^{-1}*)	*a* (*μmol CO_2 m^{-2} s^{-1}*)	*c* (*radians*)	*PTR* (*hour:min*)	*NSE*
active	R_{basal}	2867	3.77 (±0.04)	0.56 (±0.05)	4.58 (±0.09)	12:30	0.043
	$R_{myc+rhizo}$	2861	2.47 (±0.05)	0.38 (±0.06)	2.23 (±0.13)	21:30	0.020
	R_{myc}	2846	1.23 (±0.05)	0.14 (±0.06)*	5.89 (±0.4)	7:30	0.003
	R_{rhizo}	2922	1.23 (±0.04)	0.51 (±0.05)	2.36 (±0.1)	21:00	0.033
drought	R_{basal}	781	2.80 (±0.07)	0.56 (±0.09)	4.71 (±0.16)	12:00	0.050
	$R_{myc+rhizo}$	777	1.14 (±0.06)	0.5 (±0.07)	1.57 (±0.13)	0:00	0.102
	R_{myc}	747	0.40 (±0.05)	0.08 (±0.05)*	0.26 (±0.44)	5:00	0.007
	R_{rhizo}	904	0.79 (±0.03)	0.44 (±0.04)	1.7 (±0.1)	23:30	0.118
fall	R_{basal}	2304	2.63 (±0.04)	0.45 (±0.05)	4.31 (±0.09)	13:30	0.060
	$R_{myc+rhizo}$	2293	1.32 (±0.04)	0.24 (±0.05)	2.23 (±0.18)	21:30	0.016
	R_{myc}	2273	0.43 (±0.04)	0.09 (±0.05)*	1.18 (±0.41)	1:30	0.030
	R_{rhizo}	2395	0.88 (±0.02)	0.2 (±0.03)	2.49 (±0.13)	23:30	0.023
dormant	R_{basal}	777	0.90 (±0.01)	0.05 (±0.02)*	4.19 (±0.38)	14:00	0.008
	$R_{myc+rhizo}$	776	0.29 (±0.02)	0.04 (±0.03)*	1.31 (±0.48)	1:00	0.005
	R_{myc}	774	0.23 (±0.02)	0.05 (±0.02)*	5.89 (±0.52)	7:30	0.007
	R_{rhizo}	903	0.07 (±0.01)	0.06 (±0.02)*	2.23 (±0.34)	21:30	0.010

https://doi.org/10.1371/journal.pone.0223247.t003

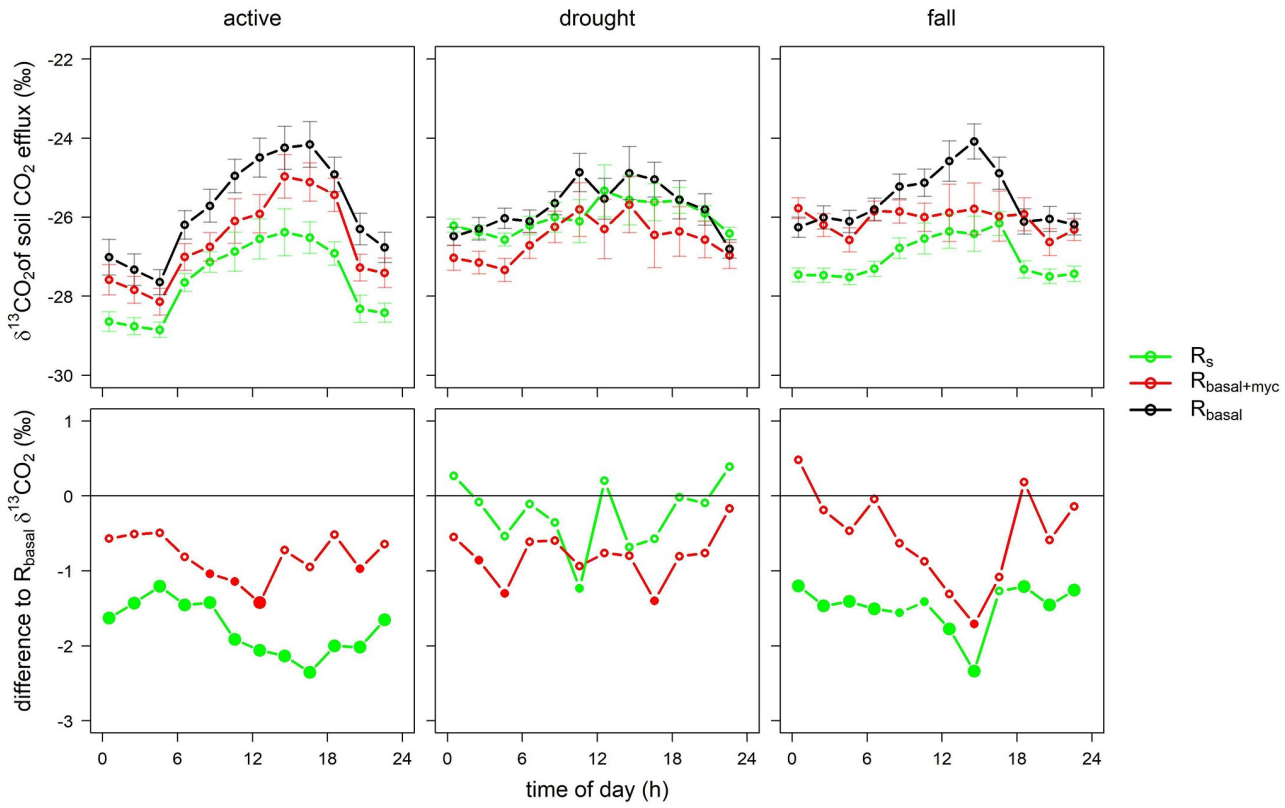

Fig 4. Diel pattern of $\delta^{13}C$ of soil CO_2 effluxes (green, red and black dots with error bars, upper panel) and the difference between $\delta^{13}C_{Rs}$ and $\delta^{13}C_{Rbasal}$ (green) and between $\delta^{13}C_{Rbasal+myc}$ and $\delta^{13}C_{Rbasal}$ (red, y = 0 represents $\delta^{13}C_{Rbasal}$, lower panel). Significant differences from $\delta^{13}C_{Rbasal}$ are shown by larger ($P<0.05$) and smaller ($P<0.1$) bold points.

https://doi.org/10.1371/journal.pone.0223247.g004

Diel pattern of $\delta^{13}C$ values of soil respiration in the phenological stages

Isotopic (^{13}C) measurements were conducted in 2013 at three phenological stages: active (from 15th May to 10th July), a drought period from 10th July to 19th August, and a fall period from 20th August to 11th November. Average $\delta^{13}C_{Rs}$ values were -27.6‰ (±1.2‰), -26.0‰ (±1.4‰), -27.0‰ (±1.0‰) (mean±SE), while average $\delta^{13}C_{Rbasal+myc}$ values were -26.6‰ (±1.5‰), -26.6‰ (±1.9‰), -26.1‰ (±1.5‰) and $\delta^{13}C_{Rbasal}$ values were -25.8‰ (±1.5‰), -25.8‰ (±1.4‰), -25.5‰ (±1.2‰) in the active, drought and fall periods, respectively. $\delta^{13}C$ data were also grouped and averaged by time of day for each phenological period (Fig 4, upper panel).

Diel pattern of $\delta^{13}C$ of all soil CO_2 effluxes was the most pronounced in the active period in all of the measured plots, and $\delta^{13}C$ of respiration was more depleted during nighttime than during daytime at all phenological stages (Fig 4 upper panel). $\delta^{13}C$ values of the reference air (chamber inlet) ranged between −16 and −8‰ and showed similar patterns with nights being more depleted than daytime periods.

The largest differences between $\delta^{13}C_{Rs}$ and $\delta^{13}C_{Rbasal}$ and between $\delta^{13}C_{Rbasal+myc}$ and $\delta^{13}C_{Rbasal}$ were also found in the active period and the diel course of these differences showed similar pattern to $R_{myc+rhizo}$ and R_{myc} during daytime (cf. Figs 2 and 5). The highest deviation of $\delta^{13}C_{Rs}$ from $\delta^{13}C_{Rbasal}$ was observed in the afternoon and evening (12:30–20:30), while the lowest deviation was observed in early morning (2:30–8:30). During the drought period $\delta^{13}C_{Rs}$ values were between $\delta^{13}C_{Rbasal}$ and $\delta^{13}C_{Rbasal+myc}$ and the diel changes of $\delta^{13}C$ were not

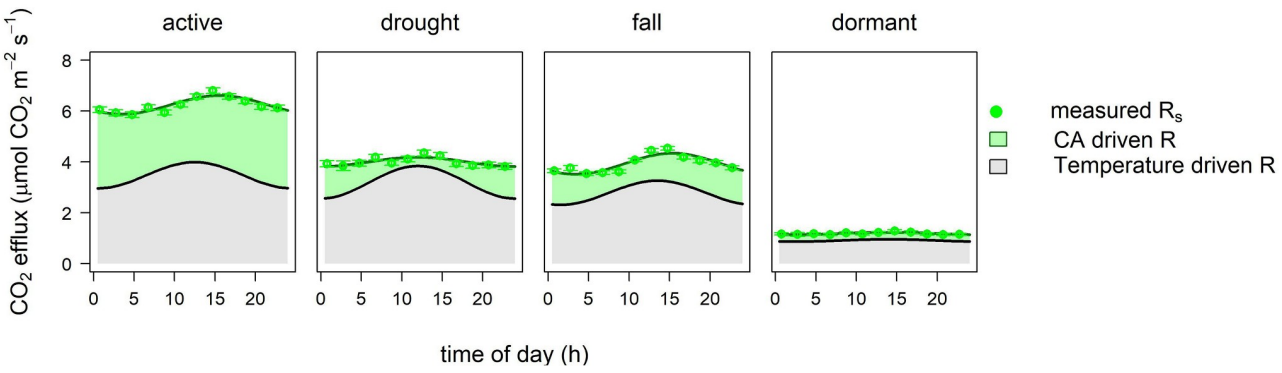

Fig 5. Conceptual model of temperature and carbon allocation driven parts of soil respiration based on Eq 5. The share of temperature driven respiration (gray area) and carbon allocation driven rhizospheric respiration (green area), as well as measured R_s averages with standard errors (green dots with error bars) are shown.

https://doi.org/10.1371/journal.pone.0223247.g005

pronounced, while the patterns observed in the active period returned in fall. $\delta^{13}C_{Rs}$ values were significantly different from $\delta^{13}C_{Rbasal}$ in the active and fall periods, while $\delta^{13}C_{Rbasal+myc}$ showed significant differences from $\delta^{13}C_{Rbasal}$ in only a few cases (Fig 4, lower panel).

Discussion

The disturbance of the soil structure in mesh-collar (root/mycorrhiza exclusion) studies is an inevitable part of the procedure and necessitates the exclusion of data of the initial period from evaluation. In order to avoid the artifacts due to the installation procedure the measurements did not start until 10 months following the installation of the tubes. At the end of the measurements we found higher hyphal density in $R_{basal+myc}$ plots than in R_s plot [39] and the absence of roots in R_{basal} and $R_{basal+myc}$ plots was also verified. Moreover, the lack of roots resulted in higher soil moisture in $R_{basal+myc}$ and R_{basal} plots than in R_s plot [39]. These differences could cause the overestimation of R_{myc} values, while R_{basal} was probably underestimated due to the exclusion of fresh SOM supply (no dead roots in the plot) and the lack of rhizodeposits accelerating SOM decomposition [33]. Soil temperature at a depth of 5 cm was also higher in R_{basal} plots than in R_s plots. Due to these differences between the plots it was not possible to use $R_{basal+myc}$ and R_{basal} respiration rates as direct estimations of heterotrophic and mycorrhizal fungi respiration. Instead, we used the calculated $R_{myc+rhizo}$, R_{rhizo} and R_{myc} rates as references to study the diel pattern of the mycorrhizal fungi and rhizospheric components of soil respiration. Since R_{basal} had no connection with the plants we could assume that the diel changes of R_{basal} were driven by the temperature. By subtracting R_{basal} from R_s we removed this temperature effect and could use $R_{myc+rhizo}$ to study the effect of carbon allocation.

The effect of carbon allocation on diel pattern of R_s

The time lag between R_s and its drivers was studied in different ecosystems and on multiple time scales [18,27]. Some studies found that the rate of photosynthesis had a stronger effect on root respiration than changes in temperature did [19,27,47]. Based on the daily averages of GPP and R_s we found 0 day lag between them in the most active period (May-July) indicating that the time lag was shorter than one day [39]. Labelling studies using stable isotopes of carbon also found short-term (<1 day) coupling between photosynthetic uptake of CO_2 and soil respiration [17,48]. However, temporal changes in photosynthetic substrate supply to the rhizosphere may also be apparent in heterotrophic respiration after a time lag [6,14]. Tracer amount peaked 24 hours after pulse-labelling in decomposer fungi and bacteria in a study by

De Deyn et al.[49]. Therefore, the observed time lag between GPP and $R_{myc+rhizo}$ included the response of the whole mycorrhizosphere. In this study $R_{basal+myc}$ always peaked earlier than R_{basal} in all phenological periods suggesting that mycorrhizal fungi respiration also had a diel pattern, which is not temperature dependent. By subtracting R_{basal} from $R_{basal+myc}$ we were able to remove the temperature effect from the diel pattern, allowing us to observe the single effect of carbon allocation on R_{myc}. This component peaked in the morning 13–20 hours after GPP peak. Similarly, the diel pattern of R_{rhizo} could also show this effect in the rhizosphere. R_{rhizo} peak preceded $R_{myc+rhizo}$ peak by 0.5–3.5 hours and R_{myc} peak by 5.5–10.5 hours in all phenological periods but it must be noted that R_{rhizo} included the respiration of rhizospheric organisms as well and not just that of the roots. Therefore, root respiration might have even shorter time lag with GPP than R_{rhizo}, i.e. less than 8–12 hours (Fig 3).

Based on the observed order of component peaks we can assume that the newly assimilated carbon induced a propagating pattern of root—rhizosphere microorganisms—mycorrhizal fungi respiration within 24 hours. The magnitude of this effect could be apparent in the amplitude of the fitted models (e.g. amplitude of $R_{myc+rhizo}$), while the remaining part of the respiration could be fueled by stored carbohydrates. Root-stored photosynthates can buffer the changes in respiration during the decline in the supply of photosynthates not only in the long run [50] but on diel scale as well [6]. Transitory starch also plays an important role as substrate for nocturnal respiration balancing the substrate supply of the rhizosphere [48]. Moreover, considerable rhizospheric priming effect could be presented only in R_s plot containing roots since root exudates are the main fuel of the process and can act in the vicinity of roots [33]. Besides the effect of carbon allocation, the observed diel pattern of R_s could partly be attributed to the link between water transport and CO_2 flux within the plants. It was recently found that CO_2 transported in the transpiration stream could reduce apparent root respiration [51,52], i.e. CO_2 production in the soil [37]. We hypothesize that all of these effects could result in the relatively low diel variability of R_s. Average diel range of respiration ($2\times a$, Eq 4) compared to the average respiration rate ($y0$, Eq 4) was higher in R_{basal} plot (40% in drought period) than in R_s plot, which varied between 8% (dormant) and 21% (fall). Diel range of R_s was small even under drought conditions (10%).

Effects of drought on diel patterns of R_s

All types of measured soil CO_2 effluxes (R_s, $R_{basal+myc}$, R_{basal}) decreased under dry conditions but the biggest decline was observed in soil respiration (R_s). Only this plot included all of the autotrophic components thus this strong response could be attributed to the autotrophic part of soil respiration. This finding is in line with previous studies where reduced autotrophic respiration was found in grassland ecosystems as a response to drought [19,48] due to the reduced assimilate supply and to the changes in allocation strategy [17]. The change in R_{myc} also supports this finding since it had much higher share in $R_{basal+myc}$ in the active period than during the drought suggesting a disproportionate reduction of carbon allocation into roots and root-associated organisms. Carbon transfer to mycorrhizal fungi could vary several-fold seasonally [16] and drought can induce increased allocation of carbon to root storage at the expense of root respiration [17,48]. Increased time lag between GPP peak and $R_{myc+rhizo}$ under drought (+2.5 hours as compared to the active period) can also be explained by this process and by the reduced speed of carbon allocation [17].

Contrary to our expectations, the amplitude of R_s was small in the drought period as compared to the amplitude of R_{basal} resulting in large diel amplitude of $R_{myc+rhizo}$ (44% of mean $R_{myc+rhizo}$). This phenomenon could only partly be attributed to the changes in the photosynthetic supply due to the small GPP in this period. Although the amount of transitory starch

declines, the increased contribution of storage pools in root respiration [6,53] could reduce this amplitude. However, the effect of another factor could also modify this diel pattern. While average diel changes of soil moisture were not significant, even a small decrease in the level of moisture in the rhizosphere could cause a decline in CO_2 efflux under water shortage. Daytime moisture depletion of the rhizosphere due to evapotranspiration could significantly affect respiration rates with rapid decline of R_s being found under 6% SWC in this ecosystem in our former studies [39,5]. Moreover, most CO_2 production takes place close to the surface (0–8 cm) in this ecosystem [37] and this upper layer is the most exposed to the daytime drying—nighttime rewetting (dew formation, water redistribution) cycles.

Diel changes in isotopic signal ($\delta^{13}C$) of soil respired CO_2

A C4 grass (*Cynodon dactylon*) was also present in the study site potentially modifying the $\delta^{13}C$ of the respired CO_2. Its cover was about 10% in the pasture [35], but it was less frequent (i.e. less than 5%) in the experimental area. Modelling results showed a strong decline in the autotrophic components in response to drought [31,39], although the observed shift (increase) in $\delta^{13}C_{Rs}$ during drought was also coincident with the maximum abundance of this species in July-August.

Uncertainties related to field measurements of isotopic signals of soil CO_2 efflux were also reported [54,55,56]. The observed diel pattern of $\delta^{13}C$ of respiration (more depleted during nights) can be explained by the effect of the non-steady-state conditions in the soil profile due to the nighttime increase of CO_2 concentration over the surface [57]. Drying of the surface layers can also modify $\delta^{13}CO_2$ since heterotrophic respiration could be restricted to the deeper layers of the soil [56]. These effects can be considerable at the study site where still conditions often occur during nighttime and dry conditions are also frequent in the vegetation period [47]. However, we can assume that all plots (R_s, $R_{basal+myc}$, R_{basal}) were affected similarly by these conditions, therefore the observed diel changes in the difference between $\delta^{13}C_{Rs}$ and $\delta^{13}CR_{basal}$ and in the difference between $\delta^{13}C_{Rbasal+myc}$ and $\delta^{13}CR_{basal}$ could be governed by the diel changes in the contribution made by rhizospheric and mycorrhizal fungi to R_s. These changes in the isotopic signals were most pronounced in the active period. The largest deviation of $\delta^{13}C_{Rs}$ from $\delta^{13}CR_{basal}$ was observed in the afternoon, following the peak in GPP by a few hours delay (~4 hours), while it was the closest to $\delta^{13}CR_{basal}$ at early morning. The largest deviation of $\delta^{13}C_{Rbasal+myc}$ from $\delta^{13}CR_{basal}$ was observed in the morning, roughly coincident with the GPP peak (-2-0 hours). Beside the changes in the component's contribution to soil respiration, post-carboxylation fractionation could also cause changes in the isotopic signal of the rhizospheric and mycorrhizal fungi components [57]. Phloem sugars can be ^{13}C enriched during night-time, while ^{13}C depleted during day-time due to the isotope fractionation of enzymatic reactions [58]. Thus, our observations in terms of the diel pattern of isotopic signals also support that the carbon uptake and root respiration have short-term (few hours) coupling, i.e. carbon allocation is fast to the roots, while it takes more time (~20–24 hours) to reach and affect the respiration of mycorrhizal fungi [49].

The integrated effects of temperature and carbon allocation govern diel variability of R_s

We used a combined sine wave model (Eq 5) to estimate the share of temperature-driven and carbon allocation driven parts of soil respiration (Fig 5). The presented conceptual model of the superposed responses could describe the causes behind the diel variability of the soil CO_2 efflux. We assume that this short-term coupling of the two processes (carbon allocation and

temperature effects) could be typical in grasslands, where the speed of the phloem transport and the short distance could induce changes in soil CO_2 efflux on the same day [14,59].

According to our model, the temperature was the major factor affecting soil respiration on the diel time scale in every phenological stages. The effect of carbon allocation was most pronounced in the active period reaching 45% share in soil respiration.

Our model concept does not separate the autotrophic and the heterotrophic components of soil respiration. More importantly, however, it separates the temperature- and the carbon allocation driven parts of the respiration, with the temperature driven part including both the heterotrophic and autotrophic response. Similarly, the carbon allocation driven part includes some heterotrophic respiration (priming) due to the root exudation in the rhizosphere [34].

Conclusions

Our results suggest that belowground carbon allocation can influence the diel pattern of soil respiration in grasslands. Based on the observed time lags between GPP and soil respiration components we can assume that the newly assimilated carbon induced a propagating pattern of root—rhizosphere microorganisms—mycorrhizal fungi respiration within 24 hours. Although temperature had the strongest effect on soil respiration according to our model, carbon allocation clearly modified the temperature driven pattern of soil respiration in the growing season. Therefore, even the time-lagged apparent temperature responses of soil respiration could contain significant respiration activities not driven by the temperature. Besides temperature and carbon allocation, soil moisture could also have an effect on the diel scale by the reduction of the autotrophic component during drought and also by the modification of the carbon allocation pattern.

Supporting information

S1 Fig. Schematic map of the study area.
(JPG)

S2 Fig. Normalized diel pattern of measured R_s values in the active period, modelled temperature driven respiration, modelled carbon allocation driven respiration and modelled soil respiration.
(JPEG)

S3 Fig. Normalized diel pattern of measured R_s values in the drought period, modelled temperature driven respiration, modelled carbon allocation driven respiration and modelled soil respiration.
(JPEG)

S4 Fig. Normalized diel pattern of measured R_s values in the fall period, modelled temperature driven respiration, modelled carbon allocation driven respiration and modelled soil respiration.
(JPEG)

S5 Fig. Normalized diel pattern of measured R_s values in the dormant period, modelled temperature driven respiration, modelled carbon allocation driven respiration and modelled soil respiration.
(JPEG)

S1 Table. Number of plot average values included in modelling (N), diel sine wave model parameters with propagated uncertainties (*y0*, *a*, *c* from Eq 4 (±SE)), peak timing of respiration (PTR) and Nash–Sutcliffe coefficient (NSE) for R_s and $R_{het+myc}$, at phenological

periods.
(DOCX)

S1 File. Soil CO_2 effluxes of the measured plots and eddy-covariance derived GPP dataset, 2011–2014, Bugac site.
(CSV)

S2 File. Isotopic signals of the measured CO_2 effluxes, 2013, Bugac site.
(CSV)

Author Contributions

Conceptualization: János Balogh, Zoltán Nagy.

Data curation: Marianna Papp, Krisztina Pintér.

Formal analysis: János Balogh.

Funding acquisition: Zoltán Nagy.

Investigation: Marianna Papp, Krisztina Pintér.

Methodology: János Balogh, Szilvia Fóti, Marianna Papp, Krisztina Pintér, Zoltán Nagy.

Visualization: János Balogh, Szilvia Fóti.

Writing – original draft: János Balogh.

Writing – review & editing: János Balogh, Szilvia Fóti, Krisztina Pintér, Zoltán Nagy.

References

1. Baldocchi D, Chu H, Reichstein M. Inter-annual variability of net and gross ecosystem carbon fluxes: A review. Agric For Meteorol. Elsevier; 2018; 249: 520–533. https://doi.org/10.1016/J.AGRFORMET.2017.05.015
2. Phillips CL, Bond-Lamberty B, Desai AR, Lavoie M, Risk D, Tang J, et al. The value of soil respiration measurements for interpreting and modeling terrestrial carbon cycling. Plant Soil.; 2017; 413: 1–25. https://doi.org/10.1007/s11104-016-3084-x
3. Vargas R, Baldocchi DD, Bahn M, Hanson PJ, Hosman KP, Kulmala L, et al. On the multi-temporal correlation between photosynthesis and soil CO_2 efflux: reconciling lags and observations. New Phytol. 2011; 191: 1006–17. https://doi.org/10.1111/j.1469-8137.2011.03771.x PMID: 21609333
4. Moyano FE, Manzoni S, Chenu C. Responses of soil heterotrophic respiration to moisture availability: An exploration of processes and models. Soil Biol Biochem. Elsevier Ltd; 2013; 1–14. https://doi.org/10.1016/j.soilbio.2013.01.002
5. Balogh J, Pintér K, Fóti S, Cserhalmi D, Papp M, Nagy Z. Dependence of soil respiration on soil moisture, clay content, soil organic matter, and CO_2 uptake in dry grasslands. Soil Biol Biochem. Elsevier Ltd; 2011; 43: 1006–1013. https://doi.org/10.1016/j.soilbio.2011.01.017
6. Hopkins F, Gonzalez-Meler M a, Flower CE, Lynch DJ, Czimczik C, Tang J, et al. Ecosystem-level controls on root-rhizosphere respiration. New Phytol. 2013; 199: 339–51. https://doi.org/10.1111/nph.12271 PMID: 23943914
7. Barba J, Cueva A, Bahn M, Barron-Gafford GA, Bond-Lamberty B, Hanson PJ, et al. Comparing ecosystem and soil respiration: Review and key challenges of tower-based and soil measurements. Agric For Meteorol. 2018; 249: 434–443. https://doi.org/10.1016/j.agrformet.2017.10.028
8. Ahlström A, Raupach MR, Schurgers G, Smith B, Arneth A, Jung M, et al. The dominant role of semi-arid ecosystems in the trend and variability of the land CO_2 sink. Science (80-). 2015; 348: 895–899. https://doi.org/10.1126/science.aaa1668 PMID: 25999504
9. Nagy Z, Pintér K, Czóbel S, Balogh J, Horváth L, Fóti S, et al. The carbon budget of semi-arid grassland in a wet and a dry year in Hungary. Agric Ecosyst Environ. Elsevier; 2007; 121: 21–29. https://doi.org/10.1016/j.agee.2006.12.003

10. Van der Molen MK, Dolman AJ, Ciais P, Eglin T, Gobron N, Law BE, et al. Drought and ecosystem carbon cycling. Agric For Meteorol. Elsevier B.V.; 2011; 151: 765–773. https://doi.org/10.1016/j.agrformet.2011.01.018

11. Moyes AB, Bowling DR. Plant community composition and phenological stage drive soil carbon cycling along a tree-meadow ecotone. Plant Soil. 2016; 401: 231–242. https://doi.org/10.1007/s11104-015-2750-8

12. Burri S, Niklaus PA, Grassow K, Buchmann N, Kahmen A. Effects of plant productivity and species richness on the drought response of soil respiration in temperate grasslands. PLoS One. 2018; 13: e0209031. https://doi.org/10.1371/journal.pone.0209031 PMID: 30576332

13. Savage K, Davidson E a., Tang J. Diel patterns of autotrophic and heterotrophic respiration among phenological stages. Glob Chang Biol. 2013; 19: 1151–1159. https://doi.org/10.1111/gcb.12108 PMID: 23504892

14. Kuzyakov Y, Gavrichkova O. Review: Time lag between photosynthesis and carbon dioxide efflux from soil: a review of mechanisms and controls. Glob Chang Biol. 2010; 16: 3386–3406. https://doi.org/10.1111/j.1365-2486.2010.02179.x

15. Abramoff RZ, Finzi AC. Are above- and below-ground phenology in sync? New Phytol. 2015; 205: 1054–1061. https://doi.org/10.1111/nph.13111 PMID: 25729805

16. Högberg MN, Briones MJI, Keel SG, Metcalfe DB, Campbell C, Midwood AJ, et al. Quantification of effects of season and nitrogen supply on tree below-ground carbon transfer to ectomycorrhizal fungi and other soil organisms in a boreal pine forest. New Phytol. 2010; 187: 485–493. https://doi.org/10.1111/j.1469-8137.2010.03274.x PMID: 20456043

17. Hasibeder R, Fuchslueger L, Richter A, Bahn M. Summer drought alters carbon allocation to roots and root respiration in mountain grassland. New Phytol. 2014; https://doi.org/10.1111/nph.13146 PMID: 25385284

18. Vargas R, Detto M, Baldocchi DD, Allen MF. Multiscale analysis of temporal variability of soil CO_2 production as influenced by weather and vegetation. Glob Chang Biol. Wiley Online Library; 2010; 16: 1589–1605. https://doi.org/10.1111/j.1365-2486.2009.02111.x

19. Gomez-Casanovas N, Matamala R, Cook DR, Gonzalez-Meler M a. Net ecosystem exchange modifies the relationship between the autotrophic and heterotrophic components of soil respiration with abiotic factors in prairie grasslands. Glob Chang Biol. 2012; 18: 2532–2545. https://doi.org/10.1111/j.1365-2486.2012.02721.x

20. Lloyd J, Taylor J. On the temperature dependence of soil respiration. Funct Ecol. JSTOR; 1994; 8: 315–323. Available: http://www.jstor.org/stable/2389824

21. Reichstein M, Subke JA, Angeli AC, Tenhunen JD. Does the temperature sensitivity of decomposition of soil organic matter depend upon water content, soil horizon, or incubation time? Glob Chang Biol. 2005; 11: 1754–1767. https://doi.org/10.1111/j.1365-2486.2005.001010.x

22. Subke J-A, Bahn M. On the 'temperature sensitivity' of soil respiration: Can we use the immeasurable to predict the unknown? Soil Biol Biochem. Pergamon Press; 2010; 42: 1653–1656. https://doi.org/10.1016/j.soilbio.2010.05.026 PMID: 21633517

23. Pavelka M, Acosta M, Marek M V., Kutsch W, Janous D. Dependence of the Q_{10} values on the depth of the soil temperature measuring point. Plant Soil. 2007; 292: 171–179. https://doi.org/10.1007/s11104-007-9213-9

24. Darenova E, Pavelka M, Acosta M. Diurnal deviations in the relationship between CO_2 efflux and temperature: A case study. Catena. Elsevier B.V.; 2014; 123: 263–269. https://doi.org/10.1016/j.catena.2014.08.008

25. Pingintha N, Leclerc MY, Beasley JP Jr., Zhang G, Senthong C. Assessment of the soil CO_2 gradient method for soil CO_2 efflux measurements: comparison of six models in the calculation of the relative gas diffusion coefficient. Tellus B. 2010; 62: 47–58. https://doi.org/10.1111/j.1600-0889.2009.00445.x

26. Zhang Q, Katul G, Oren R, Daly E, Manzoni S, Yang D. The hysteresis response of soil CO_2 concentration and soil respiration to soil temperature. J Geophys Res Biogeosciences. 2015; 120: 1–14.

27. Jia X, Zha T, Wang S, Bourque CPA, Wang B, Qin S, et al. Canopy photosynthesis modulates soil respiration in a temperate semi-arid shrubland at multiple timescales. Plant Soil.; 2018; 432: 437–450. https://doi.org/10.1007/s11104-018-3818-z

28. Guan C, Li X, Zhang P, Chen Y. Diel hysteresis between soil respiration and soil temperature in a biological soil crust covered desert ecosystem. PLoS One. 2018; 13. https://doi.org/10.1371/journal.pone.0195606 PMID: 29624606

29. Moyano F, Atkin O, Bahn M, Bruhn D, Burton A, Heinemeyer A, et al. Respiration from roots and the mycorrhizosphere. In: Bahn M, Heinemeyer A, Kutsch WL, editors. Soil Carbon Dynamics: An Integrated Methodology. Cambridge University Press; 2009. pp. 234–288.

30. Högberg P. Is tree root respiration more sensitive than heterotrophic respiration to changes in soil temperature? New Phytol. 2010; 188: 9–10. https://doi.org/10.1111/j.1469-8137.2010.03366.x PMID: 20673284

31. Balogh J, Papp M, Pintér K, Fóti S, Posta K, Eugster W, et al. Autotrophic component of soil respiration is repressed by drought more than the heterotrophic one in a dry grassland. Biogeosciences. 2016; 13: 5171–5182. https://doi.org/10.5194/bg-13-5171-2016

32. Casals P, Lopez-Sangil L, Carrara A, Gimeno C, Nogués S. Autotrophic and heterotrophic contributions to short-term soil CO_2 efflux following simulated summer precipitation pulses in a Mediterranean dehesa. Global Biogeochem Cycles. 2011; 25: GB3012. https://doi.org/10.1029/2010GB003973

33. Shahzad T, Chenu C, Genet P, Barot S, Perveen N, Mougin C, et al. Contribution of exudates, arbuscular mycorrhizal fungi and litter depositions to the rhizosphere priming effect induced by grassland species. Soil Biol Biochem. 2015; 80: 146–155. https://doi.org/10.1016/j.soilbio.2014.09.023

34. Finzi AC, Abramoff RZ, Spiller KS, Brzostek ER, Darby BA, Kramer MA, et al. Rhizosphere processes are quantitatively important components of terrestrial carbon and nutrient cycles. Glob Chang Biol. 2015; 21: 2082–2094. https://doi.org/10.1111/gcb.12816 PMID: 25421798

35. Koncz P, Besnyői V, Csathó AI, Nagy J, Szerdahelyi T, Tóth Z, et al. Effect of grazing and mowing on the microcoenological composition of semi-arid grassland in Hungary. Appl Ecol Environ Res. 2014; 12: 563–575. https://doi.org/10.15666/aeer/1202_563575

36. Driessen P, Deckers J, Spaargaren O, Nachtergaele F, editors. Lecture notes on the major soils of the world. Food and Agriculture Organization (FAO); 2001.

37. Balogh J, Fóti S, Pintér K, Burri S, Eugster W, Papp M, et al. Soil CO_2 efflux and production rates as influenced by evapotranspiration in a dry grassland. Plant Soil. Springer International Publishing; 2015; 388: 157–173. https://doi.org/10.1007/s11104-014-2314-3

38. Moyano F, Kutsch W, Schulze E. Response of mycorrhizal, rhizosphere and soil basal respiration to temperature and photosynthesis in a barley field. Soil Biol Biochem. 2007; 39: 843–853. https://doi.org/10.1016/j.soilbio.2006.10.001

39. Papp M, Fóti S, Nagy Z, Pintér K, Posta K, Fekete S, et al. Rhizospheric, mycorrhizal and heterotrophic respiration in dry grasslands. Eur J Soil Biol. Elsevier; 2018; 85: 43–52. https://doi.org/10.1016/j.ejsobi.2018.01.005

40. Pintér K, Balogh J, Nagy Z. Ecosystem scale carbon dioxide balance of two grasslands in Hungary under different weather conditions. Acta Biol Hung. 2010; 61: 130–5. https://doi.org/10.1556/ABiol.61.2010.Suppl.13 PMID: 21565771

41. Koncz P, Pintér K, Balogh J, Papp M, Hidy D, Csintalan Z, et al. Extensive grazing in contrast to mowing is climate-friendly based on the farm-scale greenhouse gas balance. Agric Ecosyst Environ. 2017; 240: 121–134. https://doi.org/10.1016/j.agee.2017.02.022

42. Fratini G, Mauder M. Towards a consistent eddy-covariance processing: An intercomparison of EddyPro and TK3. Atmos Meas Tech. 2014; 7: 2273–2281. https://doi.org/10.5194/amt-7-2273-2014

43. Webb EK, Pearman GI, Leuning R. Correction of Flux Measurements for Density Effects Due to Heat and Water-vapor Transfer. Q J R Meteorol Soc. 1980; 106: 85–100.

44. Reichstein M, Falge E, Baldocchi D, Papale D, Aubinet M, Berbigier P, et al. On the separation of net ecosystem exchange into assimilation and ecosystem respiration: Review and improved algorithm. Glob Chang Biol. 2005; 11: 1424–1439. https://doi.org/10.1111/j.1365-2486.2005.001002.x

45. Nagy Z, Pintér K, Pavelka M, Darenová E, Balogh J. Carbon balance of surfaces vs. ecosystems: advantages of measuring eddy covariance and soil respiration simultaneously in dry grassland ecosystems. Biogeosciences. 2011; 8: 2523–2534. https://doi.org/10.5194/bg-8-2523-2011

46. R Core Team. R: A Language and Environment for Statistical Computing. Vienna, Austria; 2018. Available: http://www.r-project.org/

47. Heinemeyer A, Tortorella D, Petrovičová B, Gelsomino A. Partitioning of soil CO_2 flux components in a temperate grassland ecosystem. Eur J Soil Sci. 2012; 63: 249–260. https://doi.org/10.1111/j.1365-2389.2012.01433.x

48. Burri S, Sturm P, Prechsl UE, Knohl a., Buchmann N. The impact of extreme summer drought on the short-term carbon coupling of photosynthesis to soil CO_2 efflux in a temperate grassland. Biogeosciences. 2014; 11: 961–975. https://doi.org/10.5194/bg-11-961-2014

49. De Deyn GB, Quirk H, Oakley S, Ostle N, Bardgett RD. Rapid transfer of photosynthetic carbon through the plant-soil system in differently managed species-rich grasslands. Biogeosciences. 2011; 8: 1131–1139. https://doi.org/10.5194/bg-8-1131-2011

50. Aubrey DP, Teskey RO. Stored root carbohydrates can maintain root respiration for extended periods. New Phytol. 2018; 218: 142–152. https://doi.org/10.1111/nph.14972 PMID: 29281746

51. Aubrey DP, Teskey RO. Root-derived CO_2 efflux via xylem stream rivals soil CO_2 efflux. New Phytol. 2009; 184: 35–40. https://doi.org/10.1111/j.1469-8137.2009.02971.x PMID: 19674328

52. Bloemen J, McGuire MA, Aubrey DP, Teskey RO, Steppe K. Transport of root-respired CO_2 via the transpiration stream affects aboveground carbon assimilation and CO_2 efflux in trees. New Phytol. 2013; 197: 555–65.

53. Lynch DJ, Matamala R, Iversen CM, Norby RJ, Gonzalez-Meler MA. Stored carbon partly fuels fine-root respiration but is not used for production of new fine roots. New Phytol. 2013; 199: 420–430. https://doi.org/10.1111/nph.12290 PMID: 23646982

54. Nickerson N, Risk D. Physical controls on the isotopic composition of soil-respired CO_2. J Geophys Res Biogeosciences. 2009; 114: 1–14. https://doi.org/10.1029/2008JG000766

55. Kayler ZE, Ganio L, Hauck M, Pypker TG, Sulzman EW, Mix AC, et al. Bias and uncertainty of $\delta^{13}CO_2$ isotopic mixing models. Oecologia. 2010; 163: 227–34. https://doi.org/10.1007/s00442-009-1531-6 PMID: 20043179

56. Moyes AB, Gaines SJ, Siegwolf RTW, Bowling DR. Diffusive fractionation complicates isotopic partitioning of autotrophic and heterotrophic sources of soil respiration. Plant Cell Environ. 2010; 33: 1804–19. https://doi.org/10.1111/j.1365-3040.2010.02185.x PMID: 20545887

57. Brüggemann N, Gessler A, Kayler Z, Keel SG, Badeck F, Barthel M, et al. Carbon allocation and carbon isotope fluxes in the plant soil-atmosphere continuum: a review. Biogeosciences. 2011; 8: 3457–3489. https://doi.org/10.5194/bgd-8-3619-2011

58. Gessler A, Tcherkez G, Peuke AD, Ghashghaie J, Farquhar GD. Experimental evidence for diel variations of the carbon isotope composition in leaf, stem and phloem sap organic matter in Ricinus communis. Plant, Cell Environ. 2008; 31: 941–953. https://doi.org/10.1111/j.1365-3040.2008.01806.x PMID: 18331588

59. Kayler Z, Gessler A, Buchmann N. What is the speed of link between aboveground and belowground processes? New Phytol. 2010; 187: 885–888. https://doi.org/10.1111/j.1469-8137.2010.03332.x PMID: 20707852